Received: 24 March 2022 | Revised: 5 July 2022 | Accepted: 12 July 2022

DOI: 10.1002/gea.21930

RESEARCH ARTICLE

Geoarchaeology An International Journal WILEY

Diversification of lithic raw materials used by Mesolithic inhabitants of Los Canes cave (Sierra del Cuera, Eastern Asturias, Spain), and quartz crystallite size of chert as an essential indicator parameter of its provenance

Celia Marcos[1] | María de Uribe-Zorita[1] | Patricia Fernández[2] | Pedro Álvarez-Lloret[1] | Jorge Vallejo-Llano[2] | Pablo Arias[2]

[1]Dpto. Geología y Inst. de Química Organometálica "Enrique Moles", Univ. Oviedo, Oviedo, Asturias, Spain

[2]Instituto Internacional de Investigaciones Prehistóricas de Cantabria Edificio Interfacultativo, Univ. Cantabria, Santander, Cantabria, Spain

Correspondence
Celia Marcos, Dpto. Geología y Inst. de Química Organometálica "Enrique Moles," Univ. Oviedo, Jesús Arias de Velasco s/n, 33005 Oviedo, Asturias, Spain.
Email: cmarcos@uniovi.es

Scientific editing by Ryan Parish.

Funding information
Spanish State Plan for R+D (HAR2017-82557-P)

Abstract

Two types of studies were carried out on the lithic materials found in stratigraphic unit 6 of Los Canes cave used by Mesolithic human groups: (1) quantification of the retouched and nonretouched lithic materials to determine the adaptive strategy in relation to changes in the availability and technology resources and (2) crystallographic/mineralogical characterization of the nonretouched lithic materials using the RGB (R being red, G green, and B blue) code for color, transmission polarization optical microscopy, X-ray diffraction, X-ray fluorescence, infrared and Raman spectroscopies, and total organic carbon analyses. Cluster and factorial statistical analyses were performed to establish the relationship between samples. The main conclusions extracted are as follows: (1) The mobility of the inhabitants of Los Canes cave may have been very restricted, and they used local raw materials. (2) The inhabitants of Los Canes cave used chert preferentially in the elaboration of different typologies. (3) The mineralogical and elemental compositions of the chert samples from Level 6 of Los Canes cave and those from nearby outcrops are similar. (4) The crystallite size values of the tool cherts (>1000 Å) and the almost complete absence of moganite and chalcedony indicate a high degree of maturity and could belong to the Carboniferous, the period to which the cherts of the outcrops used for comparison also belong.

KEYWORDS

chert, infrared spectroscopy, Mesolithic, transmission polarization optical microscopy, X-ray diffraction, X-ray fluorescence

1 | INTRODUCTION

Management of lithic resources has remained practically unstudied on the interior slope of the Sierra del Cuera (30 km long, about 6 km from the coast, in the Asturian municipalities of Cabrales, Peñamellera Alta, and Peñamellera Baja), the location of Los Canes cave, which is the specific site studied in this investigation. On the contrary, studies of the coastal zone began in the early twentieth century, by the Count of Vega del Sella, and continue to date (Arias, 2002; Fano, 1998; González Morales, 1978; Gutiérrez Zugasti et al., 2014; Straus & Clark, 1986). On the other hand, most of the studies on lithic materials were carried out with a focus on the products obtained from the knapping process or their function; on rare occasions, the raw material has been characterized and only through macroscopic descriptions and by comparison.

The geographical and geological reconstructions allowed characterization of the environment in which these human groups moved as a geographically complex territory, with the Sierra de Cuera as a barrier between the interior and coastal deposits (Arias et al., 2016). The nearby sites in the coastal area appear to have used a mixed-subsistence system that included a high percentage of marine resources, whereas the inland sites depended mainly on hunting mountain ungulates such as chamois (*Rupicapra pyrenaica*) or ibex (*Capra pyrenaica*). In this zone, there is also a large amount of fresh water and other mineral materials such as ochre, which were fundamental in the daily life of these groups.

Although the Sierra del Cuera is a local environment abundant in plant and animal food, there are great challenges in the acquisition of raw materials due to the existence of forests, rocky areas, and rivers that are difficult to cross, considering that the sea level has undergone at least two major oscillations. The geological base of the territory provided human communities abundant possibilities for the supply of lithic raw materials. These human populations were physically placed on, or in close proximity to, potential catchment areas abundant in quartzite, limestone, quartz, and chert raw materials. The acquision of raw material depends on the distance between settlements and outcrops, and the abundance and quality of the raw materials and their capacity to be made into certain types of blanks. This relationship continues to be discussed in the organizational framework informed by optimization theory and behavioral ecology (e.g., Andrefsky, 1994, 2009; Binford, 1979, 1980; Bleed, 1986; Bousman, 1993; Elston & Kuhn, 2002; Kelly, 1995; Kuhn, 1994; Nelson, 1991; Parry & Kelly, 1987; Surovell, 2009; Torrence, 1989). According to Andrefsky (1994), if there is an abundance of lithic raw material of good workability, they can produce any kind of tool. However, when the abundance decreased, focus shifted toward the production of tools by efficient use of raw material. In situations where only low-workability raw material is available, tools and cores are mostly informal. Therefore, low availability of high quality raw materials tended to lead to an intensification of core reduction and a subsequent increase in the core-to-blank ratio (e.g., Blades, 2001; Dibble et al., 1995). The two approaches traditionally used to link chert outcrops and archaeological sites have been linear distance or distance along the optimal route. The characterization of chert tools found in the archaeological records of prehistoric sites and nearby chert outcrops is essential for determining their provenance and therefore to infer the mobility and lithic procurement strategies between populations.

The aims of the current research were as follows: (1) to quantify the remains of the lithic materials found in stratigraphic units (SUs) 6I, 6II, and 6III of Los Canes cave used by Mesolithic human groups to determine the adaptive strategy in relation to changes in the availability and technology of resources and (2) to characterize crystallographic and mineralogically representative chert tool remains from SUs 6I, 6II, and 6III of Los Canes cave (near Arangas in the Sierra del Cuera, eastern Asturias, Spain) used by Mesolithic human groups, and compare them with samples from nearby outcrops to determine possible provenance using the crystallite size of the quartz inthe chert (Marcos et al., 2021). The cave of Los Canes is an interesting location from an archaeological point of view as it is the most important inland Mesolithic site that has been found in the Cantabrian area, those investigated to date being on the coast (Arias, 2002). It is worth identifying the human mobility and lithic procurement strategies of these inhabitants, since it still remains unknown whether they maintained social and exchange relationships with other groups, if they were able to cross the Sierra del Cuera towards the coast, and so forth.

2 | GEOGRAPHICAL AND GEOLOGICAL CONTEXT OF THE STUDY AREA

Los Canes cave is located on a landing on the southern slope of the Sierra del Cuera, to the east of Asturias, at 325 m above sea level, oriented in a SE–NW direction. Its coordinates are longitude 4° 47′42′′ West and latitude 43° 19′28′′ North. The cave is 50m long and between 1 and 2 m wide, with stalagmitic formations blocking the passage to the interior areas. It is framed in the Sierra del Cuera, sheet no. 56 "Carreña-Cabrales" of the IGME Cartography 1:50,000 (I.G.M.E., 1984), on a limestone substrate from the mountains of Namurian age, which rides on Silurian and Ordovician substrates that emerge on the intermediate floor of this slope.

Archaeologically, the most interesting areas of Los Canes cave are the entrance and the final section of the passage. The entrance is open to the SE and leads to a small room approximately 7 m long and 2.5 m wide, in the center of which there is a small narrowing of 1.5 m. The archaeological deposits studied in the current study were located in this room (Arias & Pérez Suárez, 1992).

Eleven major SUs have been distinguished at Los Canes (Arias & Pérez Suárez, 1992), focusing on SU-6 in this study, as mentioned above. This SU-6 unit is divided into different subunits, from which samples have been collected: 6I, 6II, 6IIIA, 6IIIB, and 6IIIC. The age of these units and subunits is shown in Table 1, using human bone samples of dated materials. It corresponds to the Mesolithic 11,500–5000 cal BC in this area, a transitional period from the Paleolithic to the Neolithic where quartzite, quartz, and chert were

TABLE 1 Age of SU 6 subunits of Los Canes cave

SU	Dated material	Determination (BP)	2σ interval (cal BC)	1σ interval (cal BC)	μ (cal BC)
6III-A	Human bone	6930 ± 95	5990–5643	5964–5726	5824
6-III-B	Human bone	6243 ± 35	5308–5066	5303–5083	5206
6II	Human bone (feet)	7545 ± 40	6469–6260	6451–6391	6400
6II	Human bone (esqueleto)	7208 ± 38	6218–5990	6082–6017	6070
6II	Human bone (feet)	7118 ± 34	6066–5913	6025–5925	5990
6II	Human bone (feet)	6860 ± 65	5887–5631	5802–5668	5754
6II	Human bone (skeleton)	7025 ± 80	6029–5735	5990–5806	5896
6II	Human bone (skeleton)	6770 ± 65	5796–5557	5719–5629	5673
6I	Human bone	6265 ± 75	5464–5011	5318–5074	5214
6I	Human tooth	6199 ± 29	5291–5046	5212–5072	5137
6I	Deer bone	6163 ± 33	5212–5011	5208–5047	5115
6I	Human bone	6160 ± 55	5292–4949	5208–5042	5107

Abbreviations: BC, before Christ; BP, before present; cal BC, calibrated years before Christ; SU, stratigraphic unit.

found (Arias, 2002). Quartzite, limestone, and quartz are abundant in the cave environment. Chert, due to its relative scarcity in the area and its increasing use, is a more challenging material than others in the area (e.g. quartzite, limestone) to determine its geological and geographical origin and, therefore, the supply areas and possible access routes. The prospected chert outcrops in the area of the Sierra del Cuera, in general quite poorly represented, have been previously described by Marcos et al. (2021).

The geological context of Los Canes cave and the nearby outcrops (Figure 1) corresponds to the Cantabrian Zone, formed mainly by Paleozoic rocks deformed by the Variscan orogeny. During this formation, the Alpine orogeny was also involved and some structures were reactivated (especially those directed EW) such as reverse faults and thrust fault (Bahamonde et al., 2004).

During the Upper Devonian, the subsidence of the basin gave rise to the deposit of the Hermitage formation (river sandstones) and later, in the Devonian–Carboniferous transition, the Vegamián and Baleas Formations (marine sediments) were deposited. In the Carboniferous, which constitutes the system of greater extension within the Cantabrian Zone, marine sedimentation occurred, resulting in the so-called Griotte Limestone and the Mountain Limestone (currently known as Barcaliente and Valdeteja Formations) (Wagner et al., 1971). These formations receive siliceous contributions from foraminifera, algae, sponges, and echinoderms, thanks to which several formations have been differentiated: Baleas (Wagner et al., 1971), Vegamián (Compte, 1959), Alba (Compte, 1959), and Barcaliente Formations (which, in some parts of the Somiedo-Correcillas Unit, is replaced by the Cuevas Formation) (Wagner et al., 1971). The first three formations are condensed, with a maximum thickness of about 30 m, covering the time span corresponding to the Tournaisian—Arnsbergian. Furthermore, coinciding with the end of the deposit of the Alba Formation, there is a notable increase in the sedimentation rate and evident differentiation in the basin, a product of the Variscan orogenesis, with the deposit of terrigenous materials in the innermost unit (Somiedo-Correcillas Unit) and calcareous materials in the outermost unit.

3 | METHODOLOGY

3.1 | Quantification of lithic remains

The lithic tools allow us to understand the economic and paleocultural behaviors of the groups. Lithic objects, whose sources are traceable, indicate the movements within a given physical environment. The lithic materials have been differentiated into retouched and nonretouched materials, according to the criteria used by Arias Cabal (1991) and Arias (2002). The lithic remains studied have been divided by SUs. In levels SU-6III, SU-6II, and SU-6I of Los Canes cave, the materials of the lithic remains that appear (i.e., chert, quartzite, quartz, and limestone) are the same, with variations, as in the case of the chert, in terms of different colors and characteristics (red, black, gray, and pastel).

3.2 | Characterization of chert nonretouched lithic remains

A total of 23 samples of chert nonretouched lithic remains from SU-6I, SU-6II, and SU-6III of Los Canes cave have been selected for characterization by different techniques. These samples are representative of the different chert nonretouched lithic remains found in the three SU levels investigated. The level to which these samples belong, their color, and sampling code are shown in Table 2.

The chert nonretouched lithic remains were characterized by color, texture, presence of fossils, and mineral and elemental

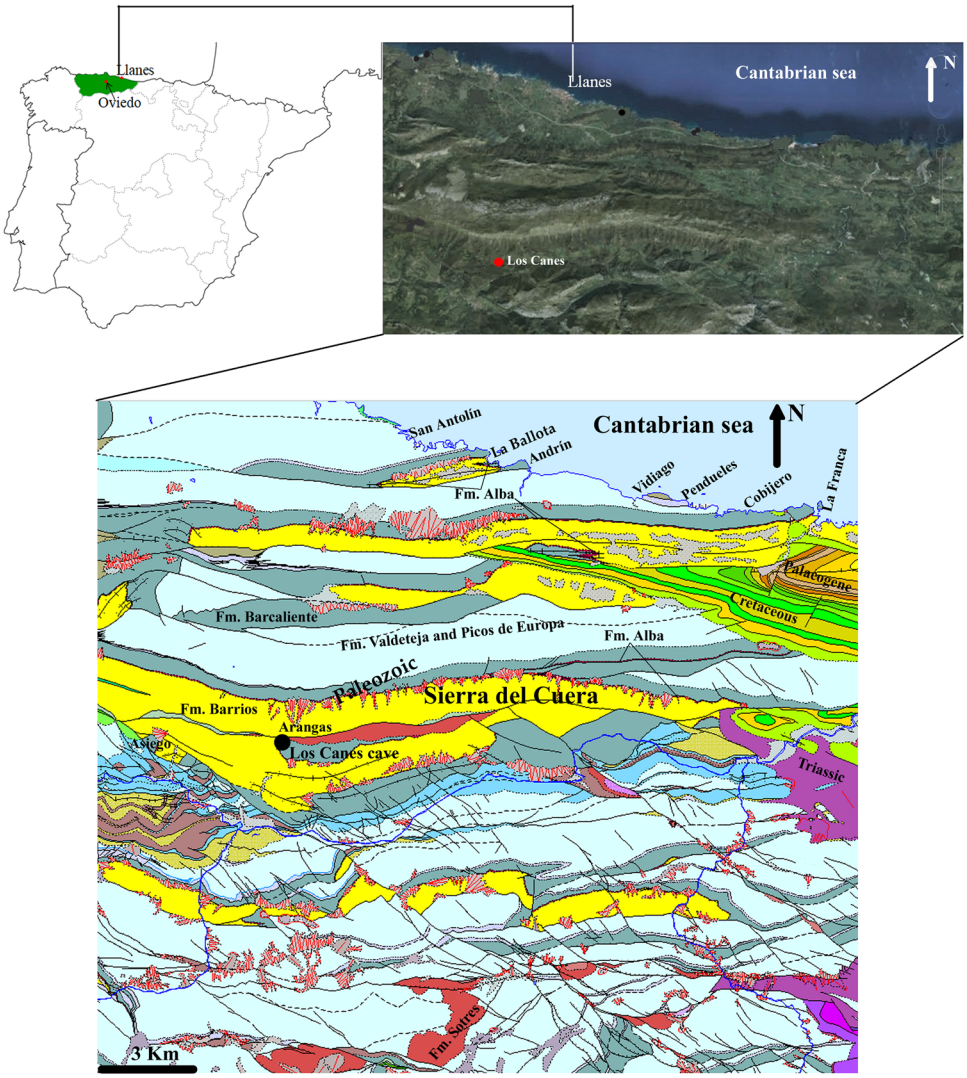

FIGURE 1 Geological context of the Los Canes cave site. ©Instituto Geológico y Minero de España (IGME) (2020). https://igme.maps.arcgis.com/home/webmap/viewer.html?webmap=44df600f5c6241b59edb596f54388ae4 March 10, 2021 (Merino-Tomé et al., 2011). [Color figure can be viewed at wileyonlinelibrary.com]

composition. Various techniques were used: RGB (R being red, G green, and B blue) color coding, transmission polarization optical microscopy, X-ray diffraction (XRD), X-ray fluorescence, infrared and Raman spectroscopies, and total organic carbon (TOC) analysis as well as statistical analysis.

3.2.1 | RGB color coding

Color is one of the most commonly used characteristics in archaeological studies to differentiate and describe chert. However, it should be taken into account that this property is difficult to determine, as it depends on many factors: the perception of the person observing it, the external light source providing the illumination, the intrinsic optical characteristics of the material observed, and the influence of the properties of the light radiations. Therefore, it will depend on the composition, structure, and texture of the chert, that is, the minerals that form the material and their grain size, since, although it has less influence, the finer it is, the more homogeneous the color will be. On the other hand, the same type of chert can show variations due to patination, leaching, or bleaching. In this study, the color of the cherts investigated was determined from the powder obtained with an agate mortar. Subsequently, the powder of each sample was photographed using the same light source and the RGB color code, and lightness (L), saturation (S), and hue (M) were obtained.

3.2.2 | Transmission polarizing optical microscopy

The transmission polarization optical microscope technique provides information on mineral composition, presence or absence of

TABLE 2 Samples of chert tool remains from Level 6 of Los Canes cave

Level		Samples	
		Color	Code
6III	A	Red	9023
		Brown	341
	B	Black	9018
		Red	8992
		Gray	8907, 8458-2, 8459-1
		Brown	9010
	C	Black	8881, 8454
		Red	5344
		Gray	8723
6II		Black	6651
		Red	3825, 4463, 7012
		Gray	4482
		Brown	3010
6I		Black	3428, 5385
		Red	3544, 6311
		Gray	5999

microfossils, and texture characteristics (size and shape of grains, presence of fractures, pores, inclusions, etc.). The microscope used was a Zeiss Axio Scope A1. For the observation of the samples, uncoated thin films were used to allow their further use in other techniques.

3.2.3 | X-ray diffraction

The XRD technique has been used to identify the crystalline phases, as well as to determine the crystallite size and lattice deformation. The samples, 0.5 g each, were previously ground in an agate mortar to obtain the diffractograms with the powder method.

This technique yields a diffractogram consisting of a series of peaks corresponding to the reflections of the crystalline planes of the phases presented in the sample. The position of the reflections in the diffractogram is conditioned by the angle θ, expressed in Bragg's law ($2d\text{sen}\theta = \lambda$, where d is the interplanar distance, θ is the diffraction angle, and λ is the wavelength of the X-rays) on which the method is based; their height and width are related to the intensity, crystallite size, and lattice deformation. The more imperfect the crystal lattice, the wider the reflections will be. These lattice imperfections are broadly classified into nanometer crystals and lattice defects (Klug & Alexander, 1974; Mittemeijer & Scardi, 2004; Snyder & Hala, 1999; Ungár, 2004; Warren, 1990).

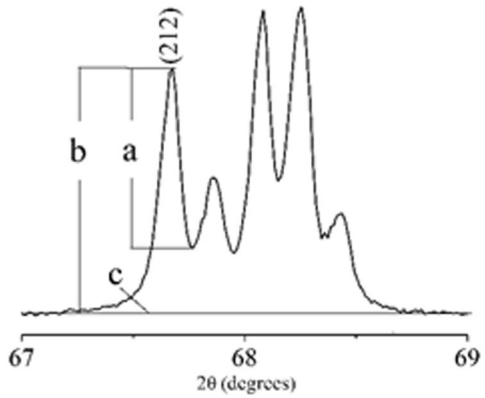

FIGURE 2 Quintet of reflections showing the (212) reflection used to calculate the crystallinity index, where "*a*" is the height of the (212) reflection, "*b*" is the height of the (212) reflection + background, and "*c*" is the background.

Phase identification has been carried out using X'Pert HighScore Plus software of the PANalytical X'pert Pro equipment. The measurement conditions were as follows: 40 mA and 45 kV, Kα-Cu radiation with $\lambda = 1.5418$ Å, 2θ range between 5° and 80°, with a 0.007° per step, and a counting time of 1 s per step. Origin Pro8.5.0 SR1 software was used to plot the diffractograms.

To evaluate the microstructural properties of the quartz domains, the full width at half maximum (FWHM) of the (101) reflection was used. Generally, two contributions to the reflection broadening can be distinguished by their different dependencies on the diffraction angle: small crystallite size and microstrain. The size of the ordered crystallites (i.e., coherently scattering domains) is limited by the interfaces, the twin boundaries, or the stacking faults. Microstrain is due to lattice imperfections such as dislocations and point defects that are associated with a stress field. The broadening caused by small crystallite size varies according to $1/\cos\theta$ (θ = incidence angle of X-rays) and the one due to lattice deformation varies according to $\beta = 4\varepsilon\tan\theta$ (β = integral reflection breadth, ε = microstrain). The α-SiO_2 standard was used for correcting the instrumental broadening. The crystallite size was obtained from the mean value of the bandwidth (FWHM) of the most intense reflection, which determines the degree of crystallinity and the order of the mineral phase, being related to the lattice deformation: As the FWHM increases, the crystallite size decreases and the lattice strain increases. It has been calculated for quartz crystal, as it is the main component of chert, by applying the Debye–Scherrer equation: *crystallite size* (Å) = $\lambda/\beta\cos\theta$, where λ is the wavelength, β is the structural broadening, and θ is the angle of incidence. The higher the crystallite size, the higher the crystallinity and the lower the lattice strain. The lattice strain (%) is given by the expression: *lattice deformation* (%) = $\beta/4\text{tg}\theta$. The crystallinity index of quartz, I_c, proposed by Murata and Norman (1975), has been

calculated. The quintet of quartz reflections with values of 2θ between 67° and 69° (2θ angle) has been used to perform the calculations, specifically by the reflection (212), at approximately 67.7° of 2θ. The height of this reflection, *a*, is divided by its total height, *b*, that is, considering the background to compensate for minor variations in the total intensity of the pattern (Figure 2). The *a*/*b* ratio is multiplied by 10 to convert fractions into numbers generally greater than 1.0.

3.2.4 | X-ray fluorescence

The chemical composition of the chert nonretouched lithic remains was determined by X-ray fluorescence using a Shimadzu EDX-720 energy-dispersive X-ray fluorescence spectrometer (XRF-EDX). This model is equipped with five types of filters for reducing and eliminating background, characteristic lines, and other types of scattered radiation. The experimental conditions used for the analyses were as follows: collimator diameter 10 mm; voltage 50 kV and current 40 μA; and measurement time of 100 s. The optimum calibration curve for the sample is selected automatically from preregistered calibration curves. The system used in this equipment does not require time-consuming pretreatment, and thin sections of chert are used. Measurements were carried out in the air because the attenuation of fluorescent X-rays is small.

The chemical composition obtained using this methodology complements the mineralogical composition of the phases identified with XRD.

3.2.5 | Total organic carbon

Due to the presence of dark spots observed by optical microscopy in all the samples analyzed, which probably correspond to organic matter, three of the samples (6I-5385, 6II-7012, and 6IIIC-5344) were selected for the measurement of TOC. These values were indirectly obtained by determining the difference between the result of total carbon (TC) and inorganic carbon (IC) analyses. The TC analysis was performed by combustion in a furnace at 900°C, and the IC analysis was performed by addition of 50% phosphoric acid in the equipment used without prior preparation of the sample received. The equipment used for these analyses was TOC-V/SSM-5000A from Shimadzu.

3.2.6 | Infrared spectroscopy

Infrared spectroscopy was used to detect vibrational modes of water, OH– groups, Si–O bonds corresponding to phases such as quartz, C–O bonds corresponding to carbonate phases such as calcite, and other bonds corresponding to other phases present in the chert nonretouched lithic remains of Los Canes cave. Infrared spectra were obtained using a JASCO 6200 (Jasco Inc.) Fourier-transform infrared spectrometer equipped with a diamond-tipped ATR Pro ONE accessory. The spectra were recorded in absorption mode at a resolution of 2 cm^{-1} over 124 scan accumulations with a spectral range of 400–4000 cm^{-1}.

3.2.7 | Raman spectroscopy

The Raman technique was used to detect the presence of moganite, a mineral phase previously revealed by XRD, in the chert nonretouched lithic remains of Los Canes cave. With this type of spectroscopy, variation in the bipolar momentum of the molecules present in the samples is not necessary for the detection of their vibration, and neither is the asymmetry, which favors precision when measuring apolar phases, as is the case of moganite, whose bonds are not bipolar, but symmetrical. Therefore, this technique is more precise than infrared spectroscopy, since, by means of vibrational spectroscopy, it is possible to identify the absorption bands of nanocrystals or even twins. Raman spectra of samples were obtained using a JASCO NRS-5100 spectrometer (Jasco Inc.) coupled to an optical Olympus microscope and equipped with an Andor DU420 classic CCD detector. Raman spectra were excited using a 785 nm red diode laser kept at 500 mW. Spectra were acquired between 100 and 1800 cm^{-1} with a resolution of 1.6 cm^{-1}, exposure time of 10 s, and 10 accumulations per measurement.

3.2.8 | Statistical analysis

Statistical analysis was carried out using IBM SPSS version 24 with data corresponding to chert nonretouched lithic remains from Level 6 of Los Canes cave and nearby outcrops previously published (Marcos et al., 2021) to make a comparison and attempt assignment of a procurement outcrop to the samples from that cave. Factor analysis was used for the interpretation of the composition of the samples. The Kaiser–Meyer–Olkin (KMO) measure of sampling adequacy and the Bartlett test of sphericity, anti-image matrix, principal component analysis as the extraction method, and Varimax with Kaiser normalization as a rotation method were used. Hierarchical clustering analysis was applied to determine the crystallite size, and the Murata index was calculated to group the data with similar properties. To obtain the groups, clusters, agglomerative clustering was used. This clustering procedure is iterative until all the data points are brought under one single larger cluster. In addition, the correlation between the crystallite size and the carbon and silicon contents, and the Murata crystallinity index, was determined using the Pearson correlation coefficient.

The most appropriate method for grouping in terms of the color, crystallite size, and the Murata index was Ward's method, with the interval-type measured distance being the most suitable. In the case of color and crystallite size, the Euclidean distance was used, and for the Murata index, the squared Euclidean distance was used.

4 | RESULTS

4.1 | Quantification of lithic remains

In levels SU-6III, SU-6II, and SU-6I of Los Canes cave, the materials of the lithic remains that appear (i.e., chert, quartzite, quartz, and limestone) are the same, with variations, as in the case of the chert, which have different colors and characteristics (red, black, gray, and pastel). The quantity of nonretouched lithic remains, weight, and average weight per piece of the lithic materials from the mentioned levels are presented in Table 3. The amount of nonretouched lithic remains and their weight vary according to the SU. In unit 6III, the number of lithic remains found was higher than those in units 6II and 6I; a decrease in the number of lithic remains was observed over time. The weight of the lithic remains and the average weight per piece were also higher in unit 6III than in the other two units investigated.

There is a high correlation between the quantity (%) of lithic remains and the weight (%) of the lithic remains. The correlation decreases for the weight (g) of lithic remains and the average weight per piece (g), and it is negative for SU-6I (Table 4).

The quantity (%), weight (%), and the average weight per piece (g) of nonretouched lithic remains of chert, quartzite, quartz, and limestone of SU-6III, SU-6II, and SU-6I are presented in Table 5. In relation to the quantity (%) and weight (%), chert predominates in the three units (≥60%). The quantity (%) of black chert predominates in units 6II and 6I and the weight (%) predominates in units 6III and 6I.

The quantity (%), weight (%), and the average weight per piece (g) of nonretouched lithic remains of chert, quartzite, quartz, and limestone from subunits A, B, and C of unit SU-6III are presented in Table 6. In relation to the quantity (%), chert predominates in the three subunits (>60%); in subunits SU-6IIIA, SU-6IIIB, and SU-6III, the weights (%) of chert and quartzite are similar. In relation to the quantity (%), gray and black chert were used slightly more than the other chert. The weight (%) of gray chert was similar in the three subunits.

The quantity of blanks made on nonretouched lithic remains of SU-6III, SU-6II, and SU-6I are presented in Table 7, and their % is presented in Table 8. The most abundant blanks in levels SU-6I, SU-6II, and SU-6III are flakes, although the other blanks tend to increase from level SU-6I, even the cores, which are very scarce. In levels SU-6III and SU-6II, chert predominates over the other lithic materials used, quartzite and quartz, for all the blanks with values higher than 40%, except in the fragments of level SU-6II, which is slightly lower. In level SU-6I, the predominant material is quartz (>50%). Limestone appears in subunit SU-6IIIC with a percentage lower than 0.5%. In relation to the type of chert, considering the color characteristic, black and gray chert predominate in the flakes of SU-6III and SU-6I units, and black and red chert predominate in the SU-6II unit. In lamellar pieces of the SU-I unit, black and gray chert are prevalent; in the SU-6II unit, black and red chert predominate and in the SU-6III unit, gray chert predominates. In the cores of the SU-I unit, gray chert dominates; in the SU-6II unit, black chert predominates and in the SU-6III unit, black and red chert predominate. In the fragments, black chert dominates in the three units. In the subunits (A, B, C) of the SU-6III unit, there are variations.

The quantity of retouched lithic objects (scrapers, perforators, burins, microliths, etc.) of SU-6I, SU-6II, and SU-6IIII, including sub-units 6IIIA, 6IIIB, and 6IIIC, is presented in Table 9, and its percentage values are presented in Table 10. There is a clear preference for the use of chert. The chert used, considering color as a characteristic, varies according to the tool type.

TABLE 3 Quantity of nonretouched lithic remains (number of specimens), weight, and average weight per piece of SU-6I, SU-6II, and SU-6IIII, including subunits 6IIIA, 6IIIB, and 6IIIC

SU	Quantity of nonretouched lithic remains	Weight (g)	Average weight per piece (g)
6IIIA	611	432.8	0.7
6IIIB	786	483.8	0.5
6IIIC	2223	1489	0.7
6III	3620	2405.6	0.6
6II	2773	935	0.3
6I	962	471.2	0.5

Abbreviation: SU, stratigraphic unit.

TABLE 4 Correlation coefficients of the quantity, weight, and average weight per piece of the nonretouched lithic remains for SU-6III, SU-6II, and SU-6I

SU	Correlation coefficient	
	Quantity (%) vs. weight (%) of lithic remains	Lithic remains weight (g) vs. average weight per piece (g)
6III	0.9	0.8
6II	0.9	0.6
6I	1	−0.5

Abbreviation: SU, stratigraphic unit.

4.2 | Characterization of the chert nonretouched lithic remains

4.2.1 | RGB color coding

The powder color of the chert samples analyzed and their corresponding RGB code are listed in Figure 3, in which it can be observed that the chert colors include shades of red, pastel, gray, and black.

TABLE 5 Quantity (%), weight (%), and the average weight per piece (g) of lithic remains of Ch, Q, Qz, and L of SU-6III, SU-6II, and SU-6I

SU	Raw material		Quantity (%)	Weight (%)	Average weight per piece (g)
6III	Ch	r	18	25	1.0
		b	31	40	0.7
		g	31	19	0.3
		p	6	2	0.3
		n.d.	15	14	0.5
	Ch		62	48	0.6
	Q		27	46	1.1
	Qz		10	6	0.3
	L		0	0	0.3
6II	Ch	r	41	49	0.3
		b	51	38	0.2
		g	4	10	0.6
		p	3	2	0.2
		n.d.	1	0	0.0
	Ch		60	52	0.3
	Q		17	36	0.6
	Qz		23	12	0.2
	L		0	0	0.0
6I	Ch	r	15	26	0.8
		b	43	51	0.6
		g	24	16	0.3
		p	5	2	0.2
		n.d.	13	5	0.2
	Ch		63	60	0.4
	Q		22	31	0.7
	Qz		15	10	0.3
	L		0	0	1.2

Abbreviations: b, black chert; Ch, chert; g, gray chert; L, limestone; n.d., nondetermined chert; p, pastel chert; Q, quartzite; Qz, quartz; r, red chert; SU, stratigraphic unit.

TABLE 6 Quantity (%), weight (%), and average weight per piece (g) of nonretouched lithic remains of Ch, Q, Qz, and L of SU-6IIIA, SU-6IIIB, and SU-6IIIC

SU	Raw material		Quantity (%)	Weight (%)	Average weight per piece (g)
6IIIA	Ch	r	10	11	0.8
		b	14	23	1.2
		g	18	10	0.4
		p	6	3	0.3
		n.d.	13	7	0.4
	Ch		61	55	0.6
	Q		28	41	1.0
	Qz		10	4	0.3
	L		0	0	0.0
6IIIB	Ch	r	11	34	1.5
		b	24	13	0.3
		g	37	19	0.3
		p	4	3	0.4
		n.d.	23	31	0.6
	Ch		61	49	0.6
	Q		27	47	1.1
	Qz		11	4	0.2
	L		0	0	0.0
6IIIC	Ch	r	20	24	0.6
		b	35	48	0.7
		g	29	18	0.3
		p	6	1	0.4
		n.d.	10	9	0.4
	Ch		63	46	0.5
	Q		26	47	1.2
	Qz		10	7	0.4
	L		0	0	1.0

Abbreviations: b, black chert; Ch, chert; g, gray chert; L, limestone; n.d., nondetermined chert; p, pastel chert; Q, quartzite; Qz, quartz; r, red chert; SU, stratigraphic unit.

4.2.2 | Transmission polarizing optical microscopy

Microphotographs of the chert nonretouched lithic remains from Los Canes cave in thin section under a transmission polarizing microscope are presented in Figure 4. The main siliceous phase observed in all chert is quartz. The presence of banding, elongation, veins, and fractures filled with calcite, and microfossils (probably radiolarians and spicules) are common. Chert from pelagic sediments has abundant radiolarian from waters with high organic productivity. In addition, dark spots probably composed of organic matter were also observed.

4.2.3 | X-ray diffraction

XRD patterns of selected samples from the analyzed chert from SU-6I, SU-6II, and SU-6III of Los Canes cave are presented in Figure 5. Chert nonretouched lithic remains of Los Canes cave show quartz as the predominant phase (JCPDS card no. 46-1045). Calcite (JCPDS card no. 5-586) is present in most of the samples. It is difficult to confirm the presence of moganite due to the overlapping of some of its reflections, (022) (3.33Å), ($\bar{1}$41) (2.29 Å), (004) (2.13 Å), (200) (2.45 Å), with those of quartz. Additional reflections in moganite such

TABLE 7 Quantity of blanks of r, b, g, p, Ch, Q, Qz, and L of SU-6III, SU-6II, and SU-6I, and the quantity of blanks of the investigated chert types

Type of remains	SU		Ch				Ch	Q	Qz	L
			b	r	g	p				
Flakes	6III	A	49	36	49	21	155	125	23	0
		B	49	27	58	5	139	121	38	1
		C	46	48	49	55	48	56	28	20
	6III		46	49	44	51	46	59	33	20
	6II		73	78	72	70	75	293	39	0
	6I		90	87	82	71	86	330	82	0
Lamellar pieces	6III	A	6	10	12	8	36	9	1	0
		B	14	9	37	7	67	16	4	0
		C	60	44	84	18	206	42	12	1
	6III		12	16	19	23	16	7	4	20
	6II		8	9	28	20	65	4	2	0
	6I		6	7	12	25	50	5	1	0
Cores	6III	A	4	2	0	2	8	0	0	0
		B	1	2	1	1	5	1	1	0
		C	6	6	2	2	16	3	5	0
	6III		2	3	0	4	2	0	2	0
	6II		0	0	0	0	0	0	0	0
	6I		0	0	1	0	0	0	2	0
Fragments	6III	A	31	25	42	18	117	23	61	0
		B	45	31	46	35	157	36	51	0
		C	41	34	31	21	127	36	65	60
	6III		40	32	36	23	36	34	61	0
	6II		19	13	0	10	15	42	59	0
	6I		5	7	5	4	5	21	14	0

Abbreviations: b, black chert; Ch, chert; g, gray chert; L, limestone; p, pastel chert; Q, quartzite; Qz, quartz; r, red chert; SU, SU, stratigraphic unit.

as ($\bar{1}21$) (3.39 Å), (110) (4.45 Å), (101) (4.38 Å), and (002) (4.26 Å) are very weak and therefore difficult to appreciate, especially if the content of this phase is very low.

Crystallite size, lattice strain, and the crystallinity index of Murata for the quartz of the chert nonretouched lithic remains from the SU-6 of Los Canes cave are presented in Table 11.

4.2.4 | X-ray fluorescence

The weight percentages of the elemental oxides analyzed with ED-XRF of the chert tool samples (mean values ± SD) are presented in Table 12. The obtained chemical composition using this methodology complements the mineralogical composition of the phases identified by XRD. The detection of SiO_2 indicates the presence of a siliceous phase, such as quartz, and other silicate phases, such as mica and feldspar, together with Al_2O_3 and K_2O. The detection of CaO indicates the presence of calcite, and similarly, the detection of Fe_2O_3 could correspond to iron oxides, such as hematite, along with SO_3 and pyrite. Sulfur could also be part of the bitumen, if present in the analyzed cherts. TiO_2 could correspond to rutile.

4.2.5 | Total organic carbon

The results of TC, IC, and TOC are shown in Table 13. The results of the analyzed carbon indicate that its origin is basically organic, although it is present in the samples analyzed in a very low percentage.

TABLE 8 Percentages of blanks of r, b, g, p, Ch, Q, Qz, and L of SU-6I, SU-6II, and SU-6III

Type of remains	SU	Ch				Ch	Q	Qz
		b	r	g	p			
Flakes	6IIIA	32	23	32	14	51	41	8
	6IIIB	35	19	42	4	47	41	13
	6IIIC	37	22	33	8	60	33	6
	6III	36	22	34	8	56	36	8
	6II	50	43	4	3	67	20	13
	6I	52	17	27	4	19	28	53
Lamellar pieces	6IIIA	17	28	33	22	78	20	2
	6IIIB	21	13	55	10	77	18	5
	6IIIC	29	21	41	9	79	16	5
	6III	26	20	43	11	78	17	4
	6II	42	39	12	7	83	10	7
	6I	33	13	39	15	17	28	55
Cores	6IIIA	50	25	0	25	100	0	0
	6IIIB	20	40	20	20	71	14	14
	6IIIC	38	38	13	13	67	13	21
	6III	38	34	10	17	74	10	15
	6II	100	0	0	0	60	40	0
	6I	0	0	100	0	14	29	57
Fragments	6IIIA	29	17	47	7	55	23	22
	6IIIB	33	11	52	4	57	27	16
	6IIIC	46	21	29	4	55	26	19
	6III	40	18	37	5	55	26	18
	6II	63	35	0	2	36	11	52
	6I	46	23	27	4	19	29	53

Abbreviations: b, black chert; Ch, chert; g, gray chert; L, limestone; p, pastel chert; Q, quartzite; Qz, quartz; r, red chert; SU, stratigraphic unit.

4.2.6 | Infrared spectroscopy

Infrared spectra of some analyzed chert nonretouched lithic remains of Los Canes cave (Figure 6) show absorption bands of the vibration modes of several bonds such as water, which, due to its intensity, shows very low content (<2%); the almost complete absence of bands corresponding to H_2O vibrational modes indicates the absence of siliceous phases such as chalcedony, a phase that was not observed in thin sections under the transmission polarization optical microscope. Absorption bands of the bonds vibration modes of quartz, with the characteristic doublet, appear between 820 and 750 cm^{-1}; below 1000 cm^{-1}, the absorption bands of the Si–O bond are present, and the

TABLE 9 Quantity of retouched lithic objects of Ch, Q, Qz, and L of SU-6III, SU-6II, and SU-6I

SU		Ch	Q	Qz
6III	A	18	0	1
	B	5	0	0
	C	16	0	0
6III		39	0	1
6II		45	6	3
6I		9	1	0

Abbreviations: Ch, chert; L, limestone; Q, quartzite; Qz, quartz; SU, stratigraphic unit.

TABLE 10 Retouched lithic objects (%) of r, b, g, p, Ch, Q, Qz, and L of SU-6I, SU-6II, and SU-6III, including subunits 6IIIA, 6IIIB, and 6IIIC

Tools type	SU		Ch				Ch	Q	Qz
			b	r	g	p			
Scraper	6III	A	0	0	0	0	0	0	0
		B	0	0	0	0	0	0	0
		C	0	0	50	50	100	0	0
	6III		0	0	50	50	100	0	0
	6II		17	33	50	0	86	14	0
	6I		100	0	0	0	100	0	0
Perforator	6III	A	0	0	100	0	100	0	0
		B	0	0	0	0	0	0	0
		C	0	0	0	0	0	0	0
	6III		0	0	100	0	100	0	0
	6II		0	0	0	0	0	0	0
	6I		0	0	0	0	0	0	0
Burin	6III	A	0	0	0	0	0	0	0
		B	0	0	0	100	100	0	0
		C	0	0	100	0	100	0	0
	6III		0	0	50	50	100	0	0
	6II		100	0	0	0	100	0	0
	6I		0	0	0	0	0	0	0
Laminite with a folded edge	6III	A	42	8	17	33	92	0	8
		B	0	50	25	25	100	0	0
		C	22	33	33	11	100	0	0
	6III		28	24	24	24	96	0	4
	6II		40	7	33	20	100	0	0
	6I		33	0	67	0	100	0	0
Notches	6III	A	0	0	0	100	100	0	0
		B	0	0	0	0	0	0	0
		C	0	50	0	50	100	0	0
	6III		0	33	0	67	100	0	0
	6II		60	20	20	0	83	17	0
	6I		50	50	0	0	67	33	0
Retouched fractures	6III	A	0	100	0	0	100	0	0
		B	0	0	0	0	0	0	0
		C	0	0	0	0	0	0	0
	6III		0	100	0	0	100	0	0
	6II		0	0	0	0	0	0	0
	6I		0	0	0	0	0	0	0

TABLE 10 (Continued)

Tools type	SU		Ch				Ch	Q	Qz
			b	r	g	p			
Geometric microliths	6III	A	0	0	0	0	0	0	0
		B	0	0	0	0	0	0	0
		C	0	0	100	0	100	0	0
	6III		0	0	100	0	100	0	0
	6II		0	0	0	0	0	0	0
	6I		0	100	0	0	100	0	0
Microburil	6III	A	100	0	0	0	100	0	0
		B	0	0	0	0	0	0	0
		C	0	0	0	0	0	0	0
	6III		100	0	0	0	100	0	0
	6II		17	0	67	17	67	11	22
	6I		0	0	0	0	0	0	0
Others	6III	A	0	0	0	100	100	0	0
		B	0	0	0	0	0	0	0
		C	0	0	0	199	100	0	0
	6III		0	0	0	100	100	0	0
	6II		0	0	0	0	0	0	0
	6I		0	0	0	0	0	0	0

Abbreviations: b, black chert; Ch, chert; g, gray chert; L, limestone; p, pastel chert; Q, quartzite; Qz, quartz; r, red chert; SU, stratigraphic unit.

presence of absorption at 695 cm^{-1} also allows identification of this mineral phase. Absorption bands of the bond vibration modes of atmospheric CO_2 at 2350 cm^{-1} are observed; and in some samples, absorption bands of the bond vibration modes of carbonate at 1405 and 870 cm^{-1} (probably calcite) are also present (Farmer, 1974). Samples with the highest amount of calcite showed more intense carbonate absorption bands.

4.2.7 | Raman spectroscopy

The Raman spectra of some chert samples, as an example, are shown in Figure 7. Furthermore, the Raman spectrum section selected between 420 and 520 cm^{-1} with the baseline subtracted for spectrometric analysis is also shown in the inset. The more intense band at ~460 cm^{-1} is associated with the presence of quartz (Kingama & Hemley, 1994; Sitarz et al., 2014), and the band visible around 500 cm^{-1} is associated with the presence of four-member rings in the moganite structure and it is the characteristic band.

4.2.8 | Statistical analysis

The results obtained using the cluster method for color, crystallite size, and the Murata index are shown in the dendrograms in Figures 8–10, respectively. The most appropriate method for performing the groupings for the three properties was Ward's method, with the interval-type measured distance being the most suitable. In the case of color and crystallite size, the Euclidean distance was used, and for the Murata index, the squared Euclidean distance was used.

The most appropriate clusters for chert color (Figure 8) are R1, R2, and R3 for red samples; G1, G2, and G3 for gray samples; B for black samples; and P1 and P2 for samples with pastel shades. However, some exceptions must be considered: the cluster analysis of sample P, dark gray to the naked eye, places it in cluster R1. The analysis of samples SA6-21 and V1, with reddish tones to the naked eye, places them in cluster P2; to this same cluster, the analysis assigns the samples of gray color 6IIIB-9010 and S-1. Sample SA1-20 with a reddish color, on analysis, is placed in cluster G2. Finally, the analysis assigns samples 6IIIA-9023 and 6I-3544 of reddish tones to cluster G1 when they should be included in cluster R3.

Four samples from Los Canes cave are included in one of the red color groups; sample 6IIIC-8454 belongs to the black group (B) and the rest belong to the gray groups.

The result of the cluster analysis of crystallite size using the Ward method and the Euclidean distance in the measurement range is shown in Figure 9; dendrograms in which the clusters are considered to be the most appropriate are 1°) up to ~1000 Å; 2°) up to 2000 Å; 3°) up to 3000 Å; 4°) up to 4000 Å; and 5°) >4000 Å.

The result of the cluster analysis of the Murata index using the Ward method and the squared Euclidean distance in the

FIGURE 3 Color and RGB parameters of chert nonretouched lithic remains from Los Canes cave. RGB, R being red, G green, and B blue. [Color figure can be viewed at wileyonlinelibrary.com]

measurement range is shown in Figure 10. For this index, the clusters considered the most appropriate are 1°) up to 2 Å; 2°) 2–3 Å; 3°) 3–4 Å; 4°) 4–5 Å; and 5°) >5 Å.

Using the factor analysis technique, the oxides of the K, Al, Ti, Fe, Ca, Mn, and Sr elements were considered as variables. The KMO measure of sampling adequacy was 0.675, indicating a strong correlation between the variables; Bartlett's test of sphericity yielded a value of 0.000, confirming the validity of the test. On the other hand, the cumulative variance in the investigated specimens was 70.5% and can be explained by two principal components. Component 1 (39.8% of the total variance) includes the following oxides: (factor loading in parentheses) K_2O (0.928), Al_2O_3 (0.925), TiO_2 (0.910), and Fe_2O_3 (0.723); Component 2 (30.7% of the total variance) is composed of CaO (0.864), MnO (0.832), and SrO (0.803).

The graphical representation of the two components is shown in Figure 11, in which Component 1 increases to the right and Component 2 to the top. Most of the chert from the outcrops and the chert nonretouched lithic remains from the cave have values of Component 1 between −1.2 and −0.25 and Component 2 between 0 and −0.8, and it is not possible to differentiate groups according to composition.

5 | DISCUSSION

The Mesolithic human groups that occupied Los Canes cave used abundant lithic materials in the area such as quartzite, limestone, and quartz as well as other more scarce but more appreciated material such as chert. However, the predisposition to preferentially use chert, despite being scarcer and more difficult to collect, can be attributed to its better quality and workability, and therefore carries a higher transportation cost (Manninen & Knutsson, 2014). Chert can be worked to produce fine cutting edges, which are difficult to obtain with quartzite, which served as an inferior substitute for these preferred materials. In addition, the coarse texture of quartzite made it less suitable for producing fine-edged tools such as knife blades and projectile tips. Quartz has some disadvantages that make it less desirable than chert or quartzite (Callahan et al., 1992; Cotterell & Kamminga, 1990; Mourre, 1996). These disadvantages are, for example, that there is a greater probability that a core made from quartz will not produce suitable blanks when needed; in addition, a quartz core has more waste than a core of another, more reliable raw material, which involves a higher transportation cost (Tallavaara et al., 2010).

The activity that needs to be carried out may influence the selection of certain local raw materials, making the use of quality

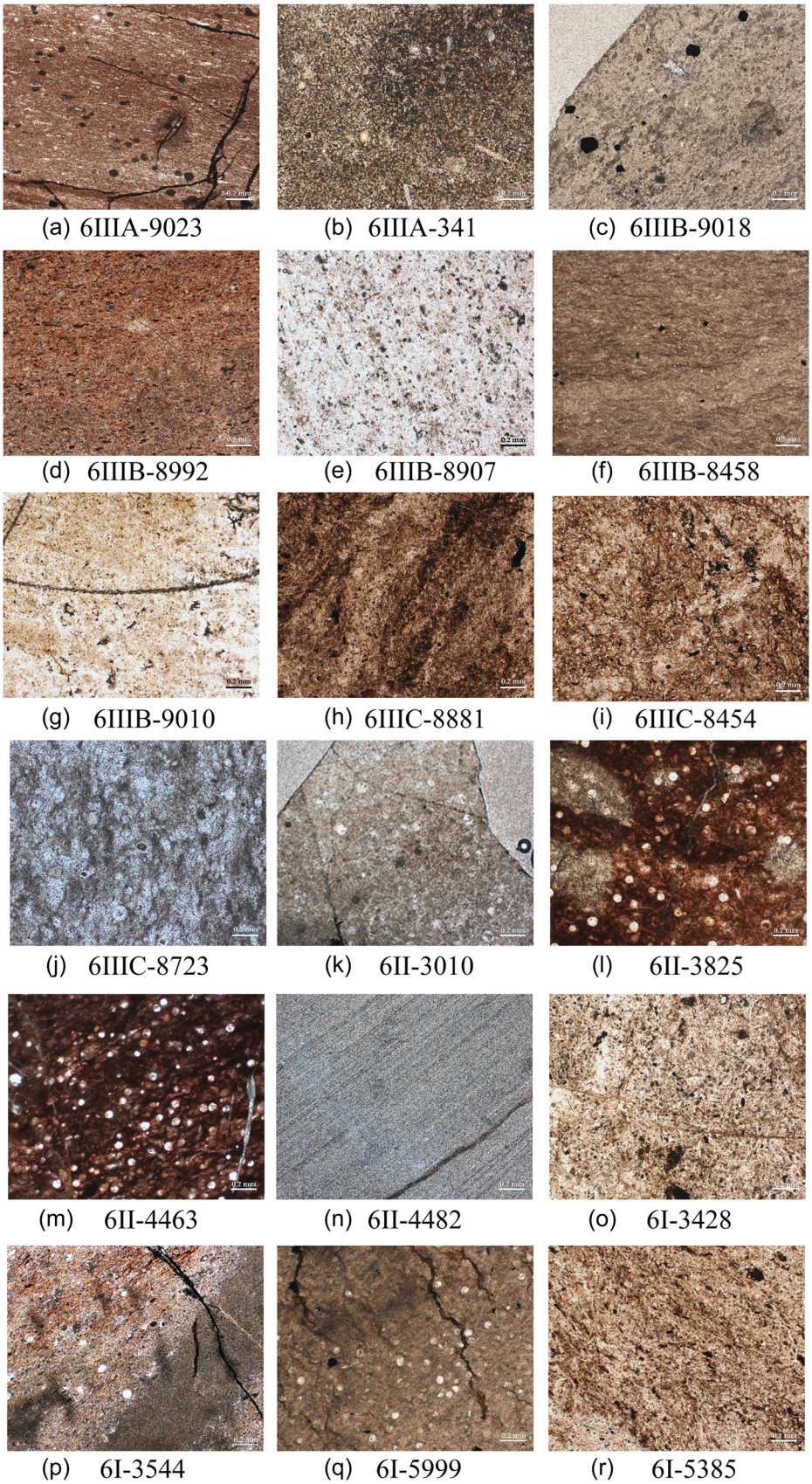

FIGURE 4 Microphotographs of the chert nonretouched lithic remains from Los Canes cave in a thin section under a transmission polarizing microscope. The white bar in each image measures 0.2 mm. [Color figure can be viewed at wileyonlinelibrary.com]

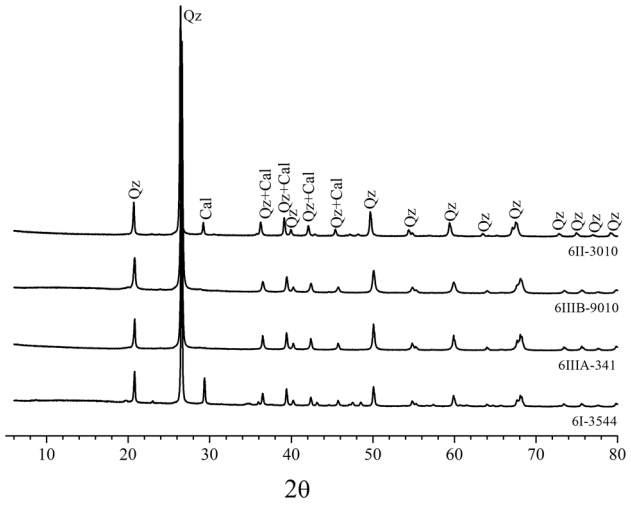

FIGURE 5 X-ray diffraction patterns of the chert nonretouched lithic remains from SU-6 of Los Canes cave showing reflections of Qz and Cal. Cal, calcite; Qz, quartz; SU, stratigraphic unit.

rocks invaluable (Cabrera Valdés et al., 2004). The use of local resources would be associated with less mobility, which could have been very restricted in the case of the inhabitants of Los Canes cave. On the other hand, it has been possible to determine the differential use of several raw materials in the elaboration of diverse lithic typologies that could have been carried out by the inhabitants of Los Canes cave.

The presence of human remains, the scarcity of cores and decortication flakes with a predominance of retouched flakes, and the low number of tools (back blades, one burin, one scraper, notches) in the investigated SUs of Los Canes cave could indicate that the cave was used for sporadic hunting and skin processing and that there existed another habitation place near the cave, such as the Arangas cave or others that have not yet been located.

Although it is still very common to assign the provenance of chert used in archaeological tools on the basis of color and textural properties, these characteristics are not sufficient, so in the last two decades, other data such as elemental and mineral phase analyses have been increasingly used (i.e., Kendall & MacDonald, 2015; Sánchez de la Torre et al., 2017). In fact, from the results obtained in this study based on color, it is deduced that it is not a determinant property to assign a specific chert to a given formation because there is high variability in its characteristic (Frederick & Ringstaff, 1994), probably related to compositional variations. However, the RGB code can represent a suitable method for analyzing the color of chert samples.

In relation to the textural characteristics, the presence of dark spots, which are probably from organic matter, banding and lineation, and microfossils, is frequent. The latter are rounded/oval, probably radiolarian, and other elongated features typical of spicules, present in some samples of tool remains analyzed from Level 6 of Los Canes cave and many of the samples analyzed from outcrops in the geological formations of Alba, Vegamián, and Barcaliente. These characteristics could indicate the origin of some chert tools used by Mesolithic humans inhabiting this cave.

TABLE 11 Crystallite size, lattice strain, and the crystallinity index of Murata for the quartz of the chert nonretouched lithic remains from SU-6 of Los Canes cave

Sample		Crystallite size (Å)	Lattice strain (%)	Crystallinite index I_c
6IIIA	341	3265	0.132	2.8
	9023	1275	0.231	2.3
6IIIB	8907	1074	0.258	1.5
	9010	1074	0.257	1.6
	8458-a	1275	0.258	2.4
	8458-b	1074	0.231	2.3
	8992	1074	0.257	1.6
6IIIC	8723	3265	0.132	4.0
	5344	2148	0.168	3.1
	8881	2148	0.168	3.1
	8454	1601	0.200	2.3
6II	3010	1070	0.258	1.2
	3825	3252	0.133	3.4
	4463	1070	0.259	2.1
	4482	>4000	0.235	6.7
	6651	916	0.289	2.4
	7012	1610	0.198	2.0
6I	3428	2148	0.168	3.2
	3544	1601	0.200	1.9
	6311	710	0.340	0.4
	5999	3265	0.132	6.9
	5385	1074	0.258	1.5

Abbreviation: SU, stratigraphic unit

In relation to the mineralogical composition of the chert analyzed, the absence or very minor presence of moganite would indicate that the chert of the outcrops corresponds to a period of time greater than 100 My, since moganite with time, temperature and weathering transforms into quartz (Bustillo, 2002; Heaney, 1995; Moxon et al., 2006).

In terms of crystallographic characteristics, the crystallite size of the chert samples from Los Canes cave is above 1000 Å in almost all samples, belonging to the same clusters as the samples from the nearby outcrops (Marcos et al., 2021). The microstructure of chert (crystallite size and microstrain) seems to be related to the formation mode and subsequent metamorphism (Rad von & Riech, 1979). The microcrystalline microstructure of chert becomes coarser in later stages of diagenesis (Richter et al., 1994) and finally recrystallizes to macroscopic quartz crystals. The intermediate phases such as opal or

TABLE 12 Percentage values of the elemental oxides analyzed by ED-XRF of the chert nonretouched lithic remains, with standard deviation in brackets

			SiO_2	CaO	Al_2O_3	K_2O	Fe_2O_3	TiO_2	SO_3	SrO	MnO
6III	A	341	95.40 (0.35)	–	4.49 (0.82)	–	0.08	–	0.02 (0.00)	–	–
				–		–	–	–		–	–
		9023	86.09 (0.15)	1.31	8.92 (0.36)	2.20 (0.01)	1.17	0.07	0.02 (0.00)	0.01 (0.00)	0.19 (0.00)
				–			–	–			
	B	8907	97.61 (0.17)	2.35 (0.01)	–	–	–	–	0.02 (0.00)	–	–
					–	–	–	–		–	–
		9010	90.82 (0.38)	0.03 (0.00)	8.78 (1.01)	0.25 (0.02)	0.06 (0.00)	–	–	–	–
								–	–	–	–
		8458-a	89.53 (0.16)	0.13 (0.00)	7.48 (0.35)	2.53 (0.02)	0.23 (0.00)	0.07 (0.00)	0.02 (0.00)	–	–
										–	–
		8992	97.61 (0.17)	2.35 (0.01)	–	–	–	–	0.02 (0.00)	–	–
					–	–	–	–		–	–
	C	8723	88.85 (0.16)	0.18 (0.00)	8.09 (0.34)	2.60 (0.02)	0.21 (0.00)	0.05 (0.00)	0.02 (0.00)	–	–
										–	–
		5344	81.52 (0.15)	0.22 (0.00)	9.05 (0.38)	6.71 (0.02)	2.35 (0.01)	0.13 (0.00)	0.02 (0.00)	–	–
										–	–
		8881	90.97 (0.16)	0.25 (0.00)	6.40 (0.35)	1.48 (0.01)	0.56 (0.00)	0.09 (0.00)	0.05 (0.00)	–	–
										–	–
		8454	91.55 (0.15)	0.25 (0.00)	5.62 (0.36)	1.82 (0.01)	0.50 (0.00)	0.06 (0.00)	0.04 (0.00)	–	–
										–	–
6II		4482	81.32 (0.19)	12.47 (0.01)	3.59 (0.55)	2.31 (0.02)	0.27 (0.00)	–	0.04 (0.00)	0.01 (0.00)	–
								–			–
		4463	77.80 (0.22)	12.04 (0.02)	6.25 (0.48)	1.83 (0.02)	1.49 (0.01)	0.07 (0.00)	0.02 (0.00)	0.01 (0.00)	0.31 (0.00)
		3825	71.19 (0.20)	3.05 (0.01)	11.95 (0.54)	10.83 (0.04)	2.45 (0.01)	0.19 (0.00)	–	–	(0.15)
									–	–	(0.00)
		3010	82.59 (0.24)	1.78 (0.01)	5.22 (0.55)	1.03 (0.02)	7.39 (0.01)	0.02 (0.00)	0.01	0.01	1.95 (0.01)
									–	–	
6I		5385	89.82 (0.17)	1.31 (0.00)	6.80 (0.44)	1.20 (0.01)	0.60 (0.00)	0.07 (0.00)	0.06 (0.00)	0.01 (0.00)	–
											–
		5999	84.42 (0.15)	0.19 (0.00)	10.04 (0.36)	2.78 (0.02)	2.24 (0.01)	0.11 (0.00)	0.02 (0.00)	–	0.03 (0.00)
										–	
		3544	79.75 (0.17)	8.61 (0.01)	7.93 (0.42)	2.72 (0.02)	0.79 (0.00)	0.07 (0.00)	0.02 (0.00)	–	0.11 (0.00)
										–	
		3428	86.76 (0.15)	0.17 (0.00)	8.01 (0.39)	3.73 (0.02)	0.92 (0.00)	0.17 (0.00)	0.07 (0.00)	–	–
										–	–

Abbreviation: ED-XRF, energy-dispersive X-ray fluorescence spectrometer.

TABLE 13 Percentages of analyzed carbon in the chert nonretouched lithic remains selected

Samples	TC %	IC %	TOC %
6IIIC-5344	0.84	0.57	0.28
6II-7012	0.28	0.06	0.22
6I-5385	0.30	0.06	0.24

Abbreviations: IC, inorganic carbon; TC, total carbon; TOC, total organic carbon.

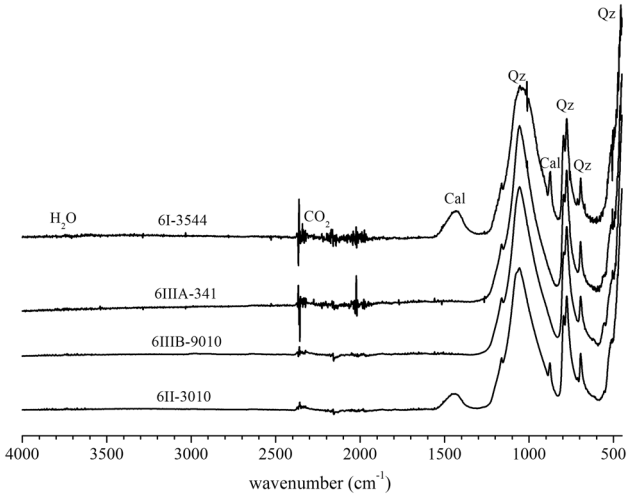

FIGURE 6 Infrared spectra of chert nonretouched lithic remains from Los Canes cave. *Note*: Qz and Cal. correspond to absorption bands of vibration modes of bonds of Qz and Cal., respectively. Cal., calcite; Qz, quartz.

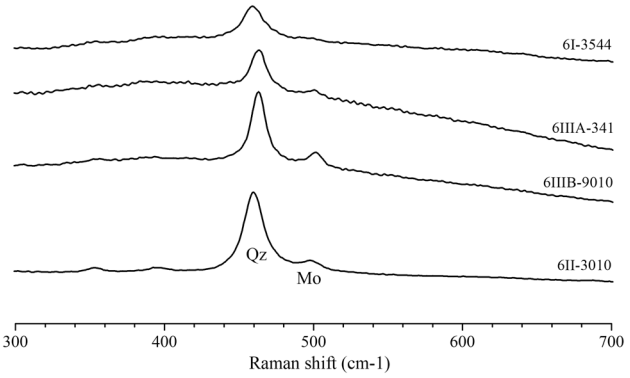

FIGURE 7 Raman spectra of the chert nonretouched lithic remains of Los Canes cave showing the bands corresponding to quartz (Qz) and moganite (Mo), respectively.

moganite are subject to changes of structural order and microstructure with time and burial depth, as demonstrated by the investigation on the gradual reduction of stacking faults in opal-CT towards opal-C with increasing diagenesis (Graetsch et al., 1994; Murata & Nakata, 1974). There is apparently a correlation between the moganite content and the size and microstrain of quartz (Graetsch & Grünberg, 2012): the moganite content is low when the crystallite size of quartz is large and microstrain is low.

The impossibility of differentiating groups by their chemical composition (obtained by XRF analyses) in the component analysis indicates that the compositions of the chert of nonretouched lithic remains from the cave and outcrops are quite similar. These compositional properties could indicate, on the one hand, a similar origin of the samples from the cave and outcrops, and on the other hand, the difficulty of specific assignment of the supply outcrops.

The TOC analyses show that the carbon is mainly of organic origin, although the percentage is very low, as expected.

Infrared spectroscopy results show the lack of water in the samples, corroborating the absence of chalcedony. The detection of moganite by this technique is not possible due to its dipolar behavior. In contrast, the presence of the band at 500 cm^{-1} in the Raman spectra of the analyzed samples confirms, without a doubt, the occurrence of moganite. On comparing the relationship of the intensities of the bands associated with moganite and quartz in the Raman spectra with that published (Bustillo, 2002; Schmidt et al., 2013), it could be concluded that the moganite content is less than 4%, which means that the period of chert maturation is high (Graetsch & Grünberg, 2012). This fact would suggest that the moganite content in the chert samples from the cave could be even lower than 4%, since its detection by XRD is practically imperceptible. Thus, the absence or almost complete absence of moganite, the crystallite size, and the microstrain of the quartz would be indicative of chert maturity and that the samples investigated from the cave belong to the same geological period as those from the outcrops, which are considered Carboniferous. Taking into account these considerations, the almost complete lack of moganite in the chert samples from Los Canes cave as well as the low microstrain and the high crystallite size of the constituent quartz are justified.

In addition to presenting different colors, the outcrop chert, even those of the same origin, have different textures and crystallographic and mineralogical characteristics. The San Antolín coastal outcrop is the one with the greatest diversity of chert. Certain textural characteristics (banding and lineation, microfossils, and organic matter) are typical of formations such as Alba, although they have spatial variations, and together with crystallographic parameters (crystallite size) and mineralogical composition, enable the identification of the origin of samples of remains of tools used by humans. This is the case for the red sample 6II-3825, which could be classified as a supply outcrop, Asiego, located very close to the cave. The rest of the samples found in Level 6 of Los Canes cave could belong to the coastal or inland outcrops sampled in this study or other outcrops in the same area or exchanged from different areas nearby.

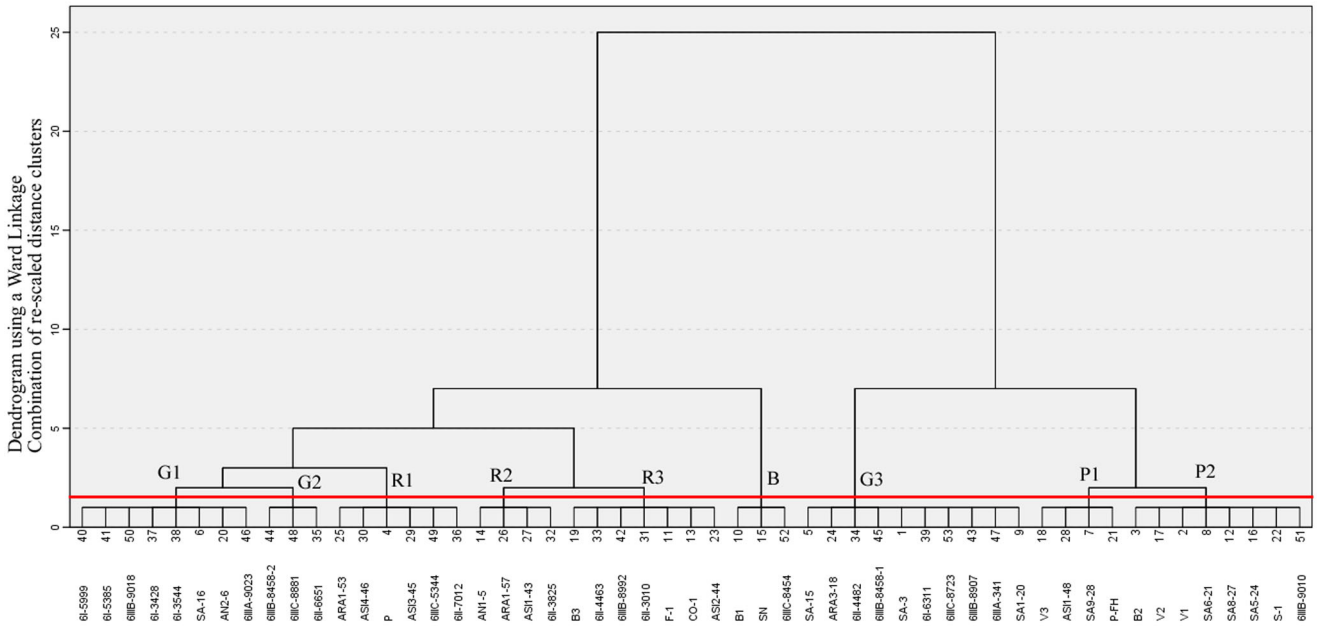

FIGURE 8 Dendrogram of the colors of the chert samples from the cave and the outcrops, using Ward's method and the Euclidean distance. The colors of each cluster are indicated: G1-G2-G3 (gray), R1-R1-R3 (red), B (black), and P1-P2 (pastel). The outcrops codes are described in Marcos et al. (2021). [Color figure can be viewed at wileyonlinelibrary.com]

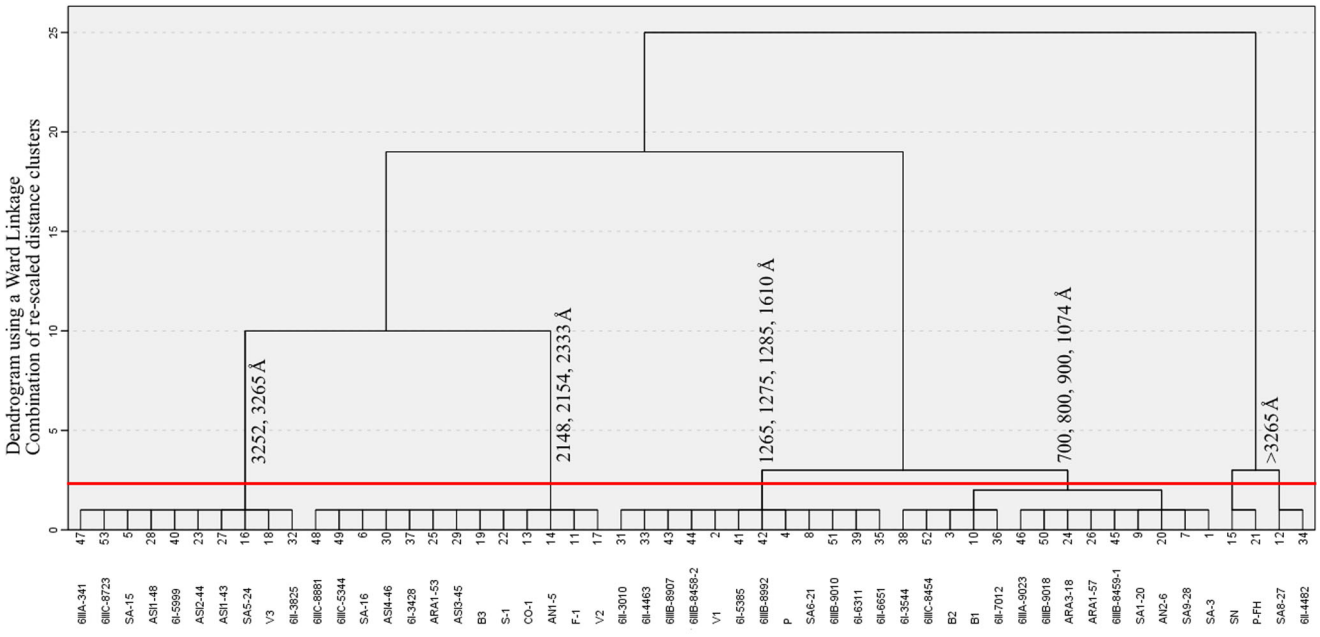

FIGURE 9 Dendrogram of the quartz crystallite sizes of the chert samples from the cave and the outcrops, using Ward's method and the Euclidean distance. The crystallite sizes of each cluster are indicated in Å. The outcrop codes are described in Marcos et al. (2021). [Color figure can be viewed at wileyonlinelibrary.com]

6 | CONCLUSIONS

The quantification and crystallographic and mineralogical characterization of the lithic remains used by the sporadic Mesolithic inhabitants of Los Canes cave have allowed us to draw the following conclusions. The mobility of the inhabitants of Los Canes cave may have been very restricted and they used local raw materials to fabricate their tools. On the other hand, it has been possible to determine the differential use of raw materials in the elaboration of different typologies by the inhabitants of Los Canes cave. They showed a tendency for preferential use of chert, even though it is scarcer and more difficult to collect.

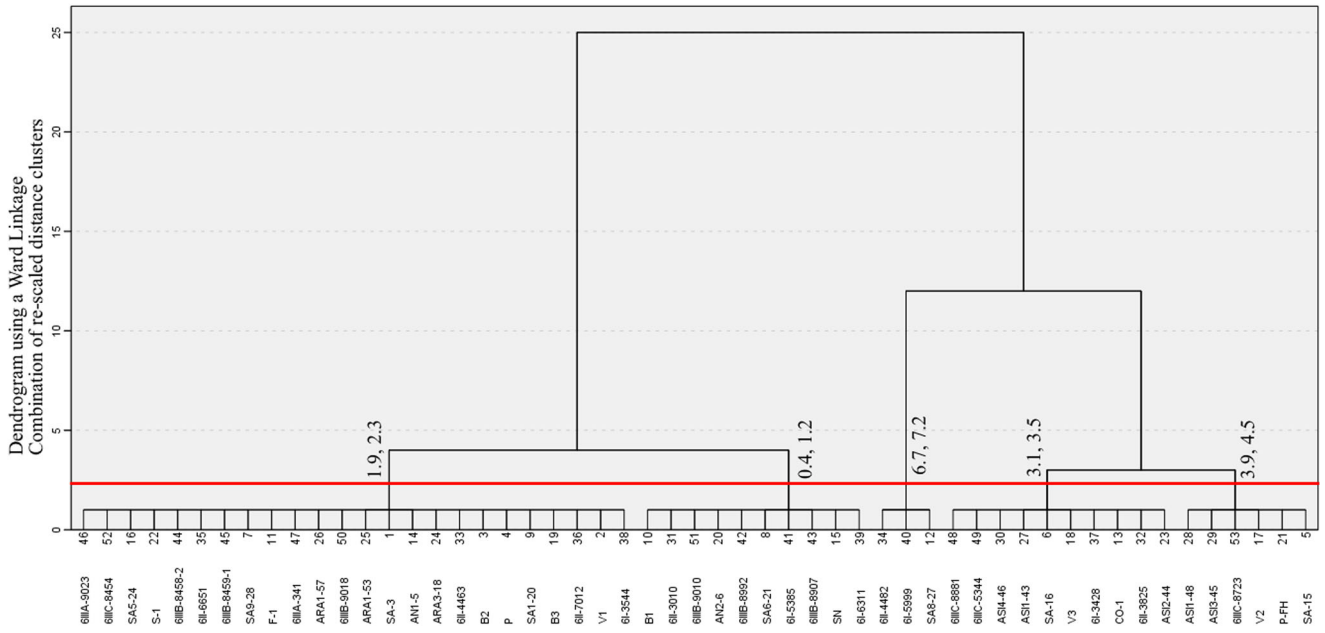

FIGURE 10 Dendrogram of the Murata index of the chert samples from the cave and the outcrops, using Ward's method and Euclidean distance squared. The Murata indices corresponding to each selected cluster are indicated. The outcrops codes are described in Marcos et al. (2021). [Color figure can be viewed at wileyonlinelibrary.com]

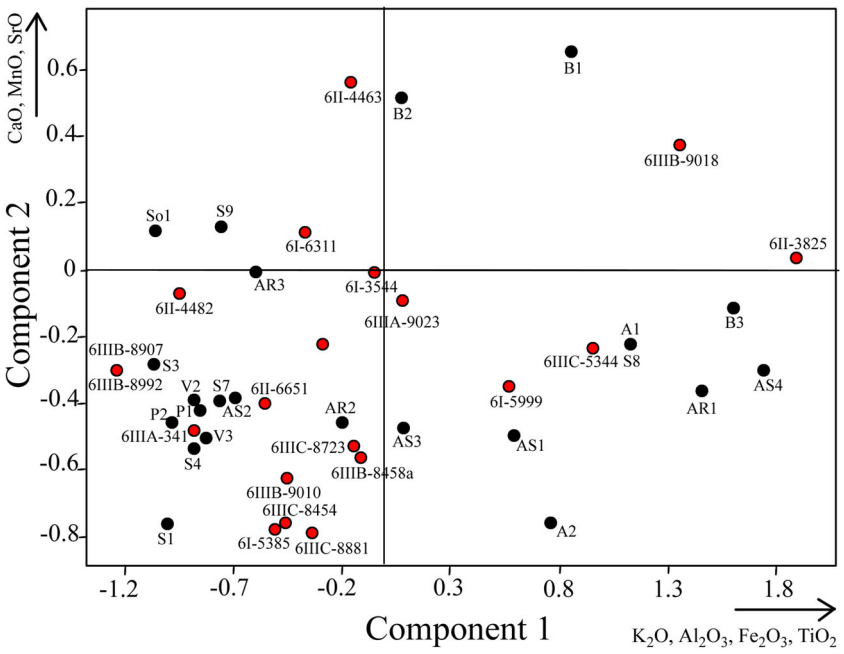

FIGURE 11 Plot of Components 1 and 2. Black dots represent the outcrops chert and red dots represent the chert nonretouched lithic remains of Los Canes cave. [Color figure can be viewed at wileyonlinelibrary.com]

The RGB color code and the cluster analysis applied to the color of the chert samples allow grouping of the samples by color, facilitating their analysis, despite the fact that this property is not a determining characteristic for assigning a chert to an outcrop.

Component analysis indicates that the mineralogical and elemental compositions of the chert samples from Level 6 of Los Canes cave and those from nearby outcrops are similar; therefore, the chert samples could come from any of the outcrops studied.

The crystallite size values of the chert from the tool remains from Level 6 of Los Canes cave, of the same order of magnitude as those from nearby coastal and inland outcrops, indicate that they could belong to the same geological period, the Carboniferous; moreover, they indicate a high degree of maturity, together with the almost complete absence of moganite and chalcedony.

Certain textural characteristics (banding and lineation, microfossils, and organic matter) are typical of formations such as Alba,

although they show spatial variations, and together with crystallographic parameters (crystallite size) and mineralogical composition, help to identify the origin of samples of remains of tools used by humans.

ACKNOWLEDGMENTS

The authors wish to acknowledge the financial support from the Spanish State Plan for R+D (HAR2017-82557-P) and also the Scientific-Technical Services of the University of Oviedo (Spain) for X-ray and energy-dispersive X-ray fluorescence techniques.

ORCID

Celia Marcos http://orcid.org/0000-0002-3208-1912

REFERENCES

Andrefsky, W. Jr. (1994). Raw-material availability and the organization of technology. *American Antiquity*, *59*(1), 21–34.

Andrefsky, W. Jr. (2009). The analysis of stone tool procurement, production, and maintenance. *Journal of Archaeological Research*, *17*, 65–103. https://doi.org/10.1007/S10814-008-9026-2

Arias Cabal, P. (1991). Estrategias de aprovechamiento de las materias primas líticas en la costa oriental de Asturias (VIII-VII milenio a. c.). In X. En Mora, X. Terradas, A. y. Parpal, & C. Plana (Eds.), *Treballs d´arqueología: Tecnología y cadenas operativas lítica* (pp. 37–55).

Arias, P. (2002). *La cueva de Los Canes (Asturias): Los últimos cazadores recolectores de la Península Ibérica ante la muerte* [Unpublished report]. Universidad de Cantabria, Santander.

Arias, P., Cubas, M., Fano, M. A., Álvarez, E., Araujo, A. C., Cueto, M., Duarte, C., Fernández, P., Iriarte, E., Jordá, J. F., López-Dóriga, I., Núñez, S., Salzmann, C., Tapia, J., Teichner, F., Teira, L. C., Uzquiano, P. Y., & Vallejo, J. A. (2016). Une nouvelle approveche pour l`étudie de l`habitat mésolithique dans le nord de la péninsule ibérique: Recherches dans le site au plein air de Alloru (Asturies, Espagne). Archéologie des chasseurscueilleurs maritimes de la fonction des habitats à l'organisation de l'espace littoral archaeology of maritime hunter–gatherers from settlement function to the organization of the coastal zone. *Actes de la Scéance de la Société Préhistorique Française Rennes*, 10–11 avril 2014.

Arias, P., & Pérez Suárez, C. (1992). Las excavaciones arqueológicas en la cueva de Los Canes (Arangas, Cabrales). Campañas de 1987 a 1990. In Gobierno del Principado de Asturias (Ed.), *Excavaciones arqueológicas en Asturias (1987:1990)* (pp. 95–110). Servicio de publicaciones del Principado de Asturias.

Bahamonde, J. R., Kenter, J. A. M., Dellaport, A. G., Keim, L., Immenhauser, A., & Reijmer, J. J. (2004). Lithofacies and depositional processes on a high, steep-margined Carboniferous (Bashkirian–Moscovian) carbonate platform slope, Sierra del Cuera, NW Spain. *Sedimentary Geology*, *166*, 145–156. https://doi.org/10.1016/j.sedgeo.2003.11.019

Binford, L. R. (1979). Organization and formation processes: Looking at curated technologies. *Journal of Anthropological Research*, *35*, 255–273.

Binford, L. R. (1980). Willow smoke and dog's tails: Hunter-gatherer settlement systems and archaeological site formation. *American Antiquity*, *45*, 4–20.

Blades, B. S. (2001). *Aurignacian lithic economy: Ecological perspectives from Southwestern France*. Kluwer Academic/Plenum Pub.

Bleed, P. (1986). Optimal design of hunting weapons. *American Antiquity*, *51*, 737–747.

Bousman, C. B. (1993). Hunter-gatherer adaptations, economic risk and tool design. *Lithic Technology*, *18*, 59–86.

Bustillo, M. A. (2002). Aparicion y significado de la moganita en fas rocas de la sílice: Una revision. *Journal of Iberian Geology*, *28*, 157–166.

Cabrera Valdés, V., Arrizabalaga, A., Bernaldo de Quirós, F., & Maillo-Fernandez, J. M. (2004). La transición al Paleolítico superior yla evolución de los contextos auriñacienses, *Las Sociedades del Paleolítico en la Región Cantábrica*. KOBIE (Serie Anejos) (Vol. 8, pp. 141–208). Diputación Foral de Bizkaia.

Callahan, E., Forsberg, L., Knutsson, K., & Lindgren, C. (1992). Frakturbilder. Kulturhistoriska kommentarer till det säregna sönderfallet vid bearbetning av kvarts. *TOR*, *24*, 27–63.

Compte, P. (1959). Recherches sur les terrains anciens de la Cordillere Cantabrique. *Memorias del Instituto Geológico y Minero de España*, *60*, 1–440.

Cotterell, B., & Kamminga, J. (1990). *Mechanics of pre-industrial technology*. Cambridge University Press.

Dibble, H. L., Roth, B., & Lenoir, M. (1995). The use of raw materials at Combe-Capelle Bas. In H. L. Dibble & M. Lenoir (Eds.), *The Middle Paleolithic Site of Cornbe-Capelle Bas (France)*. The University Museum Press.

Elston, R. G., & Kuhn, S. L. (Eds.). (2002). *Thinking small: Global perspectives on microlithization* (p. 12). Archeological Papers of the American Anthropological Association.

Fano, M. A. (1998). *El hábitat mesolítico en el Cantábrico occidental: Transformaciones Ambientales y Medio Físico durante el Holoceno Antiguo: 732 (British Archaeological Reports International Series)*. BAR Publishing.

Farmer, V. C. (Ed.). (1974). *The infrared spectra of minerals* (Vol. 4). Mineralogical Society of Great Britain and Ireland.

Frederick, C. D., & Ringstaff, C. (1994). Lithic resources at Fort Hood: Further investigations. In W. N. Trierweiler (Ed.), *Archaeological investigations on 571 prehistoric sites at Fort Hood, Bell and Coryell Counties, Texas*. Mariah Associates Inc.

González Morales, M. R. (1978). *Excavaciones en el conchero asturiense de la Cueva de Mazaculos II (La Franca, Ribadedeva, Asturias)* (pp. 369–383). Boletín del Instituto de Estudios Asturianos.

Graetsch, H., Gies, H., & Topalović, I. (1994). NMR, XRD and IR study on microcrystalline opals *Physics and Chemistry of Minerals*, *21*, 166–75.

Graetsch, H. A., & Grünberg, J. M. (2012). Microestructure of flint and other chert raw materials *Archaeometry*, *54*, 18–36.

Gutiérrez Zugasti, I., González Morales, M. R., Cuenca Solana, D., Fuertes Prieto, N., García Moreno, A. O., Menéndez, J. E., Rissetto, J., & Torres Pérez-Hidalgo, T. (2014). La ocupación de la costa durante el Mesolítico en el Oriente de Asturias: Primeros resultados de las excavaciones en la Cueva del Mazo (Andrín, Llanes). *Archaeofauna: International Journal of Archeozoology*, *23*, 25–28.

Heaney, P. J. (1995). Moganite as an indicator for vanished evaporites: A testament reborn? *Journal of Sedimentary Research*, *65*(4), 633–638.

I.G.M.E. (1984). *Mapa Geológico de España a escala 1:50.000 (1ª Serie)—Hoja 32 (LLANES)*. Escala.

Kelly, R. L. (1995). *The foraging spectrum: Diversity in Hunter–Gatherer lifeways*. Smithsonian Institution Press.

Kendall, H., & MacDonald, B. L. (2015). Chert artifact-material correlation at Keatley Creek using geochemical techniques. In T. L. Ozbun & R. L. Adams (Eds.), *Tool-stone geography of the Pacific Northwest* (pp. 49–61). Archaeology Press.

Kingama, K. J., & Hemley, R. J. (1994). Raman spectroscopic study of microcrystalline silica. *American Mineralogist*, *79*, 269–273.

Klug, H. P., & Alexander, L. E. (1974). *X-ray diffraction procedures for polycrystalline and amorphous materials* (2nd ed.). John Wiley and Songs.

Kuhn, S. L. (1994). A formal approach to the design and assembly of mobile toolkits. *American Antiquity*, *59*, 426–442.

Manninen, M. A., & Knutsson, K. (2014). Lithic raw material diversification as an adaptive strategy-technology, mobility, and site structure in

Late Mesolithic northernmost. *Europe Journal of Anthropological Archaeology*, *33*, 84–98.

Marcos, C., de Uribe–Zorita, M., Álvarez-Lloret, P., Adawy, A., Fernández, P., & Arias, P. (2021). Quartz crystallite size and Moganite content as indicators of the mineralogical maturity of the Carboniferous Chert: The case of cherts from Eastern Asturias (Spain). *Minerals*, *11*(6), 611. https://doi.org/10.3390/min11060611

Merino-Tomé, O. A., Suárez-Rodríguez, A., Alonso, J. L., González-Menéndez, L., Heredia, N., & Marcos-Vallaure, A. (2011). Mapa Geológico Digital Continuo, 1:50.000, Asturias (Zonas: 1100–1000–1600). In J. Navas, *Sistema Información Geológica Continua.[en línea]. Sistema de Información Geológica Continua: SIGECO*. En: GEODE.

Mittemeijer, E. J., & Scardi, P. (Eds.). (2004). *Diffraction analysis of the microstructure of materials* (Vol. 553). Springer Verlag.

Mourre, V. (1996). Les industries en quartz au paleolithique. Terminologie, méthodologie et technologie. *Paleo*, *8*, 205–223.

Moxon, T., Nelson, D. R., & Zhang, M. (2006). Agate recrystallisation: Evidence from samples found in Achaean and Proterozoic host rocks, Western Australia. *Australian Journal of Earth Sciences*, *53*, 235–248. https://doi.org/10.1080/08120090500499255

Murata, K. J., & Nakata, J. K. (1974). Cristobalitic stage in the diagenesis of diatomaceous shale *Science*, *184*(4136), 567–568.

Murata, K. J., & Norman, M. B. (1975). An index of crystallinity for quartz. *American Journal of Sciences*, *276*, 1120–1130.

Nelson, M. C. (1991). The study of technological organization. In M. B. Schiffer (Ed.), *Archaeological method and theory* (Vol. 3, pp. 57–100). University of Arizona Press.

Parry, W., & Kelly, R. (1987). Expedient core technology and sedentism. In J. Johnson & C. Morrow (Eds.), *The organization of core technology* (pp. 285–304). Westview Press.

Rad von, U., & Riech, V. (1979). Silica diagenesis in continental margin sediments of Northwest Africa, *Initial reports of the Deep Sea Drilling Project* (Vol. XLI, pp. 879–905). U.S. Government Printing Office.

Richter, D. K., Bruhn, F., & Wigand, R. (1994). Zur höhergradigen Chertreifung in jurassisch/alttertiären Hornsteinplattenkalken der externen Helleniden. *Zentralblatt für Geologie und Paläontologie*, *1*(7/8), 927–940.

Sánchez de la Torre, M., Le Bourdonnec, F. X., Gratuze, B., Domingo, R., García-Simón, L. M., Montes, L., Mazo, C., & Utrilla, P. (2017). Applying ED-XRF and LA-ICP-MS to geochemically characterize chert. The case of the Central-Eastern pre-Pyrenean lacus-trine cherts and their presence in the Magdalenian of NE Iberia. *Journal of Archaeological Science*, *13*, 88–98. https://doi.org/10.1016/j.jasrep.2017.03.037

Schmidt, P., Bellot–Gurlet, L., Lea, V., & Sciau, P. (2013). Moganite detection in silica rocks using Raman and infrared spectroscopy. *European Journal of Mineralogy*, *25*, 797–805. https://doi.org/10.1127/0935-1221/2013/0025-2274

Sitarz, M., Wyszomirski, P., Handke, B., & Jelen, P. (2014). Moganite in selected Polish chert samples: The evidence from MIR, Raman and X-ray studies. *Spectrochimica Acta, Part A: Molecular and Biomolecular Spectroscopy*, *122*, 55–58. https://doi.org/10.1016/j.saa.2013.11.039

Snyder, R., & Hala, J. (1999). *Defect and microstucture analysis by diffraction*. Oxford Science Publications.

Straus, L. G., & Clark, G. A. (1986). *La Riera Cave. Stone age hunter-gatherer adaptations in northen Spain. Anthropological Research papers n°36*. Arizona State University.

Surovell, T. A. (2009). *Toward a behavioral ecology of Lithic technology: Cases from Paleoindian archaeology*. The University of Arizona Press.

Tallavaara, M., Manninen, M. A., Hertell, E., & Rankama, T. (2010). How flakes shatter: A critical evaluation of quartz fracture analysis. *Journal of Archaeological Science*, *37*, 2442–2448. https://doi.org/10.1016/j.jas.2010.05.005

Torrence, R. (1989). Retooling: Towards a behavioral theory of stone tools. In R. Torrence (Ed.), *Time, energy and stone tools* (pp. 57–66). Cambridge University Press.

Ungár, T. (2004). Microstructure parameters from X-ray diffraction peak broadening. *Scripta Materialia*, *51*, 777–781. https://doi.org/10.1016/j.scriptamat.2004.05.007

Wagner, R. H., Winkler Prins, C. F., & Riding, R. E. (1971). Lithostratigraphic units of the lower part of the Carboniferons in Northern León, Spain, *Trabajos de Geología* (Vol. 4, pp. 603–663). Universidad de Oviedo.

Warren, R. E. (1990). *X-ray diffraction*. Dover Publications Inc.

How to cite this article: Marcos, C., de Uribe-Zorita, M., Fernández, P., Álvarez-Lloret, P., Vallejo-Llano, J., & Arias, P. (2022). Diversification of lithic raw materials used by Mesolithic inhabitants of Los Canes cave (Sierra del Cuera, Eastern Asturias, Spain), and quartz crystallite size of chert as an essential indicator parameter of its provenance. *Geoarchaeology*, 37, 902–922. https://doi.org/10.1002/gea.21930